Carbon Catalysis

DOI: 10.1002/anie.201006768

Phosphorus-Doped Graphite Layers with High Electrocatalytic Activity for the O_2 Reduction in an Alkaline Medium**

Zi-Wu Liu, Feng Peng, Hong-Juan Wang, Hao Yu, Wen-Xu Zheng, and Jian Yang*

The cathodic oxygen reduction reaction (ORR) is an active area of research because of its crucial role in electrochemical energy conversion in fuel cells.[1–4] One of the most attractive challenges in this area is the development of efficient ORR electrocatalysts for application in fuel cells. In the past, considerable effort has been devoted to the study of platinum and platinum-based metal alloy electrocatalysts.[5–12] Although much progress has been made, this noble metal catalyst and its alloy can hardly meet the demands which allow for widespread commercialization of fuel cells because of their sluggish electron-transfer kinetics,[13] high costs, limited supply,[14] and poor durability[15]. Platinum-free,[16–18] non-noble metal,[15,19–21] and metal-free[3,4,22,23] catalysts have been developed and evaluated to improve the performance and to reduce the costs of ORR electrocatalysts. Consequently, metal-free catalysts have attracted much interest because of their increased electrocatalytic activity inr the ORR and their better stability, and provide an opportunity to develop a new generation of catalysts. However, most of these metal-free catalysts doped with nitrogen were prepared by using metal catalysts (especially, Fe). Therefore, it is difficult to distinguish whether the catalytic activity of a carbon catalyst is caused by its unique electronic properties or by some metal residue.[24]

Phosphorus, an element of the nitrogen group, has the same number of valence electrons as nitrogen and often shows similar chemical properties. Although the electrocatalytic activity of N-doped carbon materials for the ORR has been widely investigated,[25,26] to our knowledge, there has been no report on the performance of P-doped carbon materials for the ORR. Herein, we have prepared a P-doped graphite layer catalyst without any metal residue and we examined its electrochemical properties. The results prove that this catalyst shows high electrocatalytic activity, long-term stability, and excellent tolerance to cross-over effects of methanol in the oxygen reduction reaction in an alkaline medium. Such a metal-free catalyst can not only be used as a facile and effective alternative to platinum and platinum-based catalysts for the ORR, but it allows determination of whether the electrocatalytic activity of a heteroatom-doped carbon catalyst for the ORR is caused by its unique electronic properties or by some metal residue.[27,28]

The P-doped graphite layers were prepared by pyrolysis of toluene and triphenylphosphine (TPP). In a typical experiment, a quartz tube was placed in a tubular furnace. Then, the temperature at the hot zone of the quartz tube, which was loaded in the tubular furnace, was raised to 1000 °C at an Ar flow rate of 600 mL min^{-1}. After the air in the quartz tube had been replaced by Ar, 10 mL of a toluene solution with 2.5 wt % TPP was injected close to the hot zone of the quartz tube at a flow rate of 2 mL h^{-1}, where it was vaporized and carried to the hot zone of the quartz tube by the Ar flow. To guarantee complete pyrolysis of the solution, the tubular furnace was mainteined at 1000 °C for 30 minutes after the 10 mL of the toluene solution had been conveyed completely into the quartz tube. The furnace was then cooled down to room temperature at an Ar flow rate of 100 mL min^{-1}. Afterwards, the resulting sample was collected from the inner wall of the quartz tube at the hot zone. For comparison, the carbon materials without any P dopant were synthesized by the same method using toluene.

Digital photographs and scanning electron microscopy (SEM) images have indicated that the resulting products consist of flakelike graphite layers (Figure 1 A–C and Figure S1 A–C in the Supporting Information), with some convex

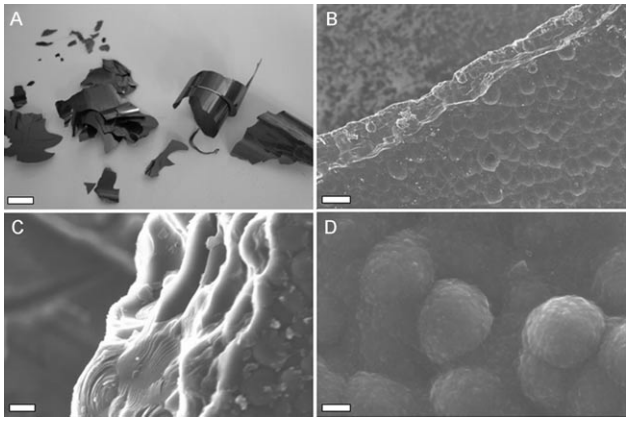

Figure 1. Digital photograph of the P-doped graphite layers collected from the quartz tube (A) and SEM images of the P-doped graphite layers (B–D). Scale bars: 1 cm (A); 20 μm (B); 1 μm (C); 200 nm (D).

[*] Dr. Z.-W. Liu, Prof. F. Peng, Dr. H.-J. Wang, Dr. H. Yu, Prof. J. Yang
School of Chemistry and Chemical Engineering
South China University of Technology
Guangzhou, Guangdong, 510640 (China)
Fax: (+86) 20-8711-4916
E-mail: cefpeng@scut.edu.cn
Dr. W.-X. Zheng
Institute of Biomaterial, College of Science
South China Agricultural University
Guangzhou, 510642 (China)

[**] This work was supported by the Fundamental Research Funds for the Central Universities of China (2009ZZ0032) and the Guangdong Provincial Natural Science Foundation of China (No. 9251064101020).

Supporting information for this article is available on the WWW under http://dx.doi.org/10.1002/anie.201006768.

caplike structures apparent on the surface of each graphite layer of the two samples (Figures 1 B,C and Figure S1 B,C in the Supporting Information). Many smaller raised caplike structures were also evident on the surface of every bigger convex cap (Figure 1 D and Figure S1 D in the Supporting Information). Raman spectroscopic analysis (Figure S2 A,B in the Supporting Information) confirmed that both samples are graphite compounds.[29] The P-doped graphite layers possess more defects in the graphitic structure (Figure S2 in the Supporting Information) than the non-phosphorus graphite layers. Successful addition of P to the graphite layers was confirmed by energy-dispersive spectrometry of the P-doped graphite layers (Figure S3 and Table S1 in the Supporting Information). X-ray photoelectron spectroscopic measurements of the P-containing sample (Figure S4 in the Supporting Information) further confirmed the incorporation of phosphorus atoms into the graphene sheets. The Brunauer–Emmett–Teller (BET) surface areas of the P-doped carbon materials and the non-phosphorus materials were almost equal, with values of 3986 and 3895 $cm^2 g^{-1}$, respectively.

To investigate the electrocatalytic activity of the P-doped graphite for the ORR we compared the electrocatalytic properties of the P-doped carbon materials with those of the bare glassy carbon (BGC) electrode, the non-phosphorus graphite layers, and a commercial platinum–carbon catalyst (Pt–C, Pt: 47.6%) by cyclic voltammetry in an aqueous solution of nitrogen-protected, air- or O_2-saturated, 0.1 M KOH solution at a scanning rate of 100 $mV s^{-1}$. The electrocatalytic performance of the BGC electrode was tested before the same amounts of P-doped graphite, non-phosphorus graphite, and Pt–C catalyst (159.1 $\mu g cm^2$) were loaded onto the BGC electrode. As shown in Figure 2 A, two signals corresponding to oxygen reduction currents were observed at about −0.44 V in an air- and O_2-saturated, 0.1 M KOH solution; such reduction currents have been reported to be the two-electron reduction process of O_2 to peroxide which is electrochemically mediated by the oxygen-containing groups at the BGC electrode surface with superoxide as an intermediate.[30] Likewise, the two signals of the oxygen reduction were also observed at about −0.40 V in the cyclic voltammograms (CVs) of the non-phosphorus graphite/GC electrode; the corresponding current densities were slightly larger than those with the BGC electrode (Figure 2 B). However, the oxygen reduction currents of the P-doped graphite/GC electrode in air- and O_2-saturated, 0.1 M KOH solutions appear as well-defined cathodic signals at about −0.30 V relative to the BGC electrode and the non-phosphorus graphite/GC electrode (Figure 2 C); a signal at −0.26 V is observed under the same conditions when an N-doped graphite electrode is used.[4] This finding strongly indicates that the phosphorus atoms have been incorporated into the hexagonal network of the sheetlike graphene structure and had the same impact as the nitrogen atoms on the electronic structure of graphite. The oxygen reduction current densities of the P-doped graphite/GC electrode were about four times higher than those of the BGC electrode and the non-phosphorus graphite/GC electrode in an oxygen-saturated 0.1 M KOH solution with an oxygen flow rate of 20 $mL min^{-1}$ (Figure 2 A,B, Table S2 in the Supporting Information); these oxygen reduction current densities are similar to those of the N-doped graphite/GC electrode and the vertically aligned nitrogen-containing carbon nanotube/GC electrode under the basic conditions.[3,4] Furthermore, the increase in the O_2 flow rate led to a clear enhancement in the diffusion current of the

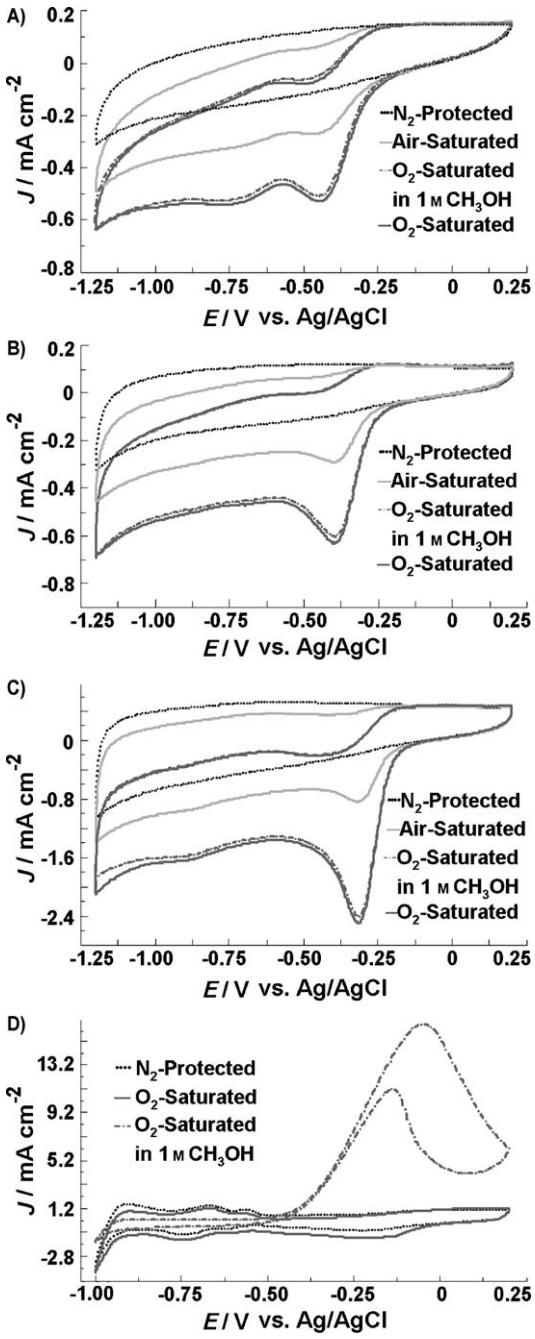

Figure 2. Typical cyclic voltammograms for the ORR at the BGC electrode (A), the non-phosphorus graphite/GC electrode (B), the P-doped graphite/GC electrode (C), and the Pt–C/GC electrode (D) in a nitrogen-protected, air-saturated, 0.10 M KOH solution, an oxygen-saturated, 0.10 M KOH solution, or an oxygen-saturated 0.1 M solution of KOH upon addition of CH_3OH (1 M) at an oxygen flow rate of 20 $mL min^{-1}$. Scan rate: 100 $mV s^{-1}$. The wavelike bands over −1.0 to −0.5 V shown for the pristine Pt–C/GC electrode may be attributed to hydrogen adsorption/desorption.

oxygen reduction (Table S2 in the Supporting Information), which suggests pronounced electrocatalytic activity of the P-doped graphite for oxygen reduction. The maximum oxygen reduction current density of the Pt–C/GC electrode at about −0.14 V was much smaller than that of the P-doped graphite/GC electrode at about −0.30 V in the same oxygen-saturated alkaline solution with an oxygen flow rate of 20 mL min^{-1} (Figure 2 C,D,). This high electrocatalytic activity of the P-doped graphite layers in the ORR can be ascribed to 1) the good electron-donor properties of phosphorus, which were calculated by the semiempirical quantum chemical method AM1,[31] and 2) to the strong electron affinity of phosphorus for positive charges (Figure S6 A,B in the Supporting Information) in the graphene sheets of the P-doped graphite; these properties facilitate the adsorption of O_2 and significantly enhance the rate of the overall oxygen reduction process.

To examine possible cross-over effects we measured the electrocatalytic selectivity of the BGC electrode, the non-phosphorus graphite/GC electrode, the P-doped graphite/GC electrode, and the Pt–C/GC electrode against the electro-oxidation of methanol—a typical fuel molecule with a cross-over property—by cyclic voltammetry in an O_2-saturated, 0.1 M KOH solution with 1 M methanol. The cathodic signals for the ORR at about −0.14 V vanished in the CV curves of the Pt–C/GC electrode when the O_2-saturated 0.1 M KOH solution was replaced by methanol (Figure 2 D). The signal intensity corresponding to methanol oxidation at the Pt–C/GC electrode even reached 16.72 mA cm^2 at −0.03 V in an O_2-saturated, 0.1 M KOH solution. However, no noticeable change was observed for the BGC electrode, the non-phosphorus graphite/GC electrode, and the P-doped graphite/GC electrode under the same conditions (Figure 2 A–C). These results indicate that the P-doped and the non-phosphorus carbon graphite catalyst possess a much higher selectivity for the ORR and a remarkably improved ability to avoid cross-over effects than the Pt–C catalyst, which means that no mixed potential will arise when the P-doped graphite catalyst is used in the direct methanol alkaline fuel cell.

To gain further insight into the role of the P-doped graphite catalyst during the ORR electrochemical process we continued to compare its electrocatalytic performance with that of the BGC electrode, the non-phosphorus graphite layers, and the commercial Pt–C catalyst by linear sweep voltammetry in an aqueous solution of O_2-saturated, 0.1 M KOH with an oxygen flow rate of 20 mL min^{-1} at a rotation rate of 1600 rpm and a scan rate of 10 mV s^{-1}. The same amount of each catalyst (101.9 μg cm^2) was loaded onto a GC rotating-disk electrode (RDE). The onset potential of the P-doped graphite/GC electrode for the ORR at approximately +0.10 V was much higher than that of the BGC electrode at about −0.11 V as well as that of the non-phosphorus graphite/GC electrode at about −0.10 V (Figure 3 A); the oxygen reduction current densities of the P-doped graphite/GC electrode were much larger than those of the BGC elctrode and the non-phosphorus graphite/GC electrode. This finding confirms that doping of phosphorus into the hexagonal network of graphene sheets changes the electronic structure of graphite to some extent. The onset potential of the P-doped graphite/GC electrode for the ORR was higher than that for the Pt–C/GC electrode at about +0.01 V, whereas the oxygen reduction current densities of the P-doped graphite/GC were lower than those of the Pt–C/GC (Figure 3 A). However, the oxygen reduction currents of the Pt–C/GC electrode dropped rapidly and they were lower than those of the P-doped graphite/GC electrode when methanol was added into the alkaline electrolyte solution (Figure 3 A line 4′). In contrast, there was no apparent change in the oxygen reduction

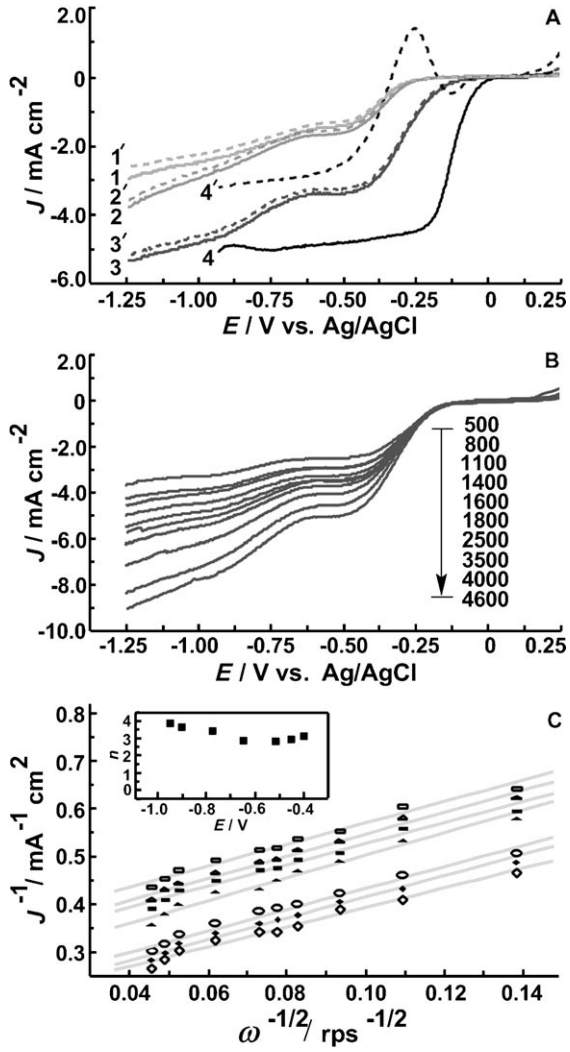

Figure 3. A) RDE voltammograms of the BGC electrode (1), the non-phosphorus graphite/GC electrode (2), the P-doped graphite/GC electrode (3), and the Pt-C/GC electrode (4) in an oxygen-saturated, 0.10 M KOH solution as well as the BGC electrode (1′), the non-phosphorus graphite/GC electrode (2′), the P-doped graphite/GC electrode (3′), and the Pt–C/GC electrode (4′) in an oxygen-saturated, 0.10 M KOH solution after addition of 1.0 M methanol at an oxygen flow rate of 20 mL min^{-1} and at a rotation rate of 1600 rpm. Scan rate: 10 mV s^{-1}. B) RDE voltammograms of the P-doped graphite/GC electrode in an O_2-saturated, 0.1 M KOH solution at an oxygen flow rate of 20 mL min^{-1}, at a scan rate of 10 mV s^{-1}, and at different rotation rates. C) Koutecky–Levich plot of J^{-1} versus $\omega^{-1/2}$ at different electrode potentials: (□) −0.40, (△) −0.45, (■)-0.51, (▲)−0.65, (○) −0.83, (◆) −0.90, and (◇) −0.95 V. The inset shows the dependence of n on the potential. The experimental data were obtained from (B).

currents at the BGC electrode, the non-phosphorus graphite/GC electrode, and the P-doped graphite/GC electrode after addition of methanol to the 0.1 M KOH solution (Figure 3A). In an actual application, the oxygen reduction current densities of the Pt–C/GC electrode were much inferior, without rotation of the cathodic electrode, to those of the P-doped graphite/GC electrode (Figure 2C,D). Furthermore, the oxygen reduction currents of the Pt–C/GC electrode were much lower than those of the heteroatom-doped carbon catalysts, when a smaller amount of the Pt–C catalyst was loaded onto the GC electrode.[3,4] Thus, the Pt–C catalyst may be replaced by the P-doped graphite catalyst when it is used in direct methanol alkaline fuel cell applications.

The oxygen reduction current density recorded at the P-doped graphite/GC electrode increased as the rotation speed increased (from 500 to 4600 rpm; Figure 3B). The Koutecky–Levich plots (I^{-1} vs. $\omega^{-1/2}$) at different electrode potentials displayed good linearity (Figure 3C), and the slopes remained approximately constant over the potential range from −0.38 to −0.95 V, which suggest that the electron transfer numbers are similar for oxygen reduction at different electrode potentials. The transferred electron number (n) per oxygen molecule involved was calculated on the basis of the Koutecky–Levich equation [Eq. (1)],[32]

$$I^{-1} = I_k{}^{-1} + (0.62nFCD^{2/3}\nu^{-1/6}\omega^{1/2})^{-1} \quad (1)$$

where I is the measured current density, I_k is the kinetic current density of the ORR, n is the overall number of electrons transferred during the oxygen reduction, F is the Faraday constant ($F = 96485\ \mathrm{C\,mol^{-1}}$), C is the bulk concentration of O_2, D is the diffusion coefficient of O_2 in the KOH electrolyte, ν is the kinetic viscosity of the electrolyte, and ω is the angular velocity of the disk ($\omega = 2\pi N$, N is the linear rotation speed). We used the values $C = 1.2\times10^{-3}\ \mathrm{mol\,l^{-1}}$, $D = 1.9\times10^{-5}\ \mathrm{cm^2\,s^{-1}}$, $\nu = 0.01\ \mathrm{cm^2\,s^{-1}}$ in 0.1 M KOH solution.[14] The dependence of n on the potential in the case of the P-doped graphite/GC electrode is shown as an inset in Figure 3C. The n value is higher than two ($n \approx 3$) in the potential range of −0.4 to −0.7 V (plateau) and increases to four at more negative potentials; this observation reveals that the peroxide is formed first and that it is then partially reduced further to water during the process of oxygen reduction. This oxygen reduction behavior of the P-doped graphite layers was supported by the presence of peroxide species in the reduction reaction (Figure S5 in the Supporting Information) and is similar to that of vertically aligned undoped carbon nanotubes in 0.1 M KOH solution.[26]

Another major concern about catalysts is their durability in fuel cell applications. To evaluate the stability of the BGC electrode, the non-phosphorus graphite, the P-doped graphite, and the commercial Pt–C catalyst we conducted tests on their stability by continuous potential cycling in an aqueous solution of O_2-saturated, 0.1 M KOH with an oxygen flow rate of $20\ \mathrm{mL\,min^{-1}}$ over 12000 cycles. The maximum oxygen reduction current density of the P-doped graphite/GC electrode was almost invariable (Figure 4), as is the case for the BGC electrode and the non-phosphorus graphite/GC electrode. The maximum current value in every CV of the P-doped graphite/GC electrode was always about four times higher than that of the BGC electrode and the non-phosphorus graphite/GC electrode; this value is much larger than that of the Pt–C/GC electrode during a continuous potentiodynamic sweep for 12000 cycles, and it shows the outstanding durability and high electrocatalytic activity of the P-containing graphite layer catalyst in the ORR and is comparable to that of a nitrogen-containing carbon catalyst in an alkaline electrolyte.[3] In contrast, the Pt–C/GC electrode exhibited a gradual decrease, with a current loss of approximately 31.4%, measured after 12000 cycles, which suggests that the stability of this noble catalyst is much inferior to that of the P-doped graphite catalyst. While the stability of noble and non-noble metal catalysts is rather unsatisfactory,[21,33] deactivation, which occurs in metal-based catalysts through loss of active metal particles from the surface of the catalyst support, is not observed in the case of heteroatom-doped carbon catalysts. This is the case because the strength of the covalent P–C and N–C bond is well above the adsorption forces exerted between the noble or non-noble metal catalysts and their supports.

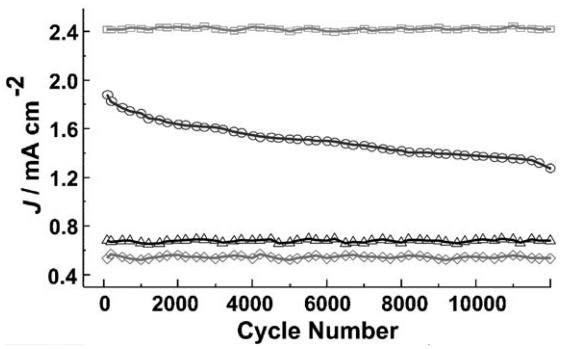

Figure 4. The maximum oxygen reduction current densities of the P-doped graphite/GC electrode (□), the Pt–C/GC electrode (○), the non-phosphorus graphite/GC electrode (△), and the BGC electrode (◇) recorded during repeated cycling.

In summary, we have demonstrated the synthesis of P-doped graphite layers by a thermolysis approach, in which toluene was used as an carbon precursor and triphenylphosphine as the phosphorus source. After successful incorporation of phosphorus into the network of graphene sheets, the resulting P-doped graphite—a typical metal-free catalyst—shows high electrocatalytic activity, long-term stability, and excellent tolerance to cross-over effects of methanol in the ORR in an alkaline medium. This type of heterodoped graphite will provide an opportunity to design and develop various metal-free, efficient ORR catalysts, which are essential for practical applications in fuel cells. Optimization and fabrication studies on P-doped graphite materials are underway.

Received: October 28, 2010
Revised: January 14, 2011
Published online: March 4, 2011

Keywords: carbon · fuel cells · metal-free catalysis · oxygen reduction · phosphorus

[1] R. Adzic, J. Lipkowski, P. N. Ross, *Electrocatalysis*, Wiley-VCH, New York, **1998**, pp. 197 – 180.
[2] B. C. H. Steele, A. Heinzel, *Nature* **2001**, *414*, 345 – 352.
[3] P. Gong, F. Du, Z. H. Xia, M. Durstock, L. M. Dai, *Science* **2009**, *323*, 760 – 764.
[4] R. L. Liu, D. Q. Wu, X. L. Feng, K. Mullen, *Angew. Chem.* **2010**, *122*, 2619 – 2623; *Angew. Chem. Int. Ed.* **2010**, *49*, 2565 – 2569.
[5] A. Kongkanand, S. Kuwabata, G. Girishkumar, P. Kamat, *Langmuir* **2006**, *22*, 2392 – 2396.
[6] J. Zhang, K. Sasaki, E. Sutter, R. R. Adzic, *Science* **2007**, *315*, 220 – 222.
[7] B. Lim, M. J. Jiang, P. H. C. Camargo, E. C. Cho, J. Tao, X. M. Lu, Y. M. Zhu, Y. N. Xia, *Science* **2009**, *324*, 1302 – 1305.
[8] B. C. Beard, P. N. Ross, *J. Electrochem. Soc.* **1986**, *133*, 1839 – 1845.
[9] G. Tamizhmani, G. A. Capuano, *J. Electrochem. Soc.* **1994**, *141*, 968 – 975.
[10] H. Yang, W. Vogel, C. Lamy, N. Alonso-Vante, *J. Phys. Chem. B* **2004**, *45*, 4211 – 4217.
[11] F. Colmati, E. Antolini, E. R. Gonzalez, *J. Power Sources* **2006**, *157*, 98 – 103.
[12] J. Zhang, H. Z. Yang, J. Y. Fang, S. H. Zou, *Nano Lett.* **2010**, *10*, 638 – 644.
[13] W. Chen, J. M. Kim, S. H. Sun, S. W. Chen, *J. Phys. Chem. C* **2008**, *112*, 3891 – 3898.
[14] W. Chen, S. W. Chen, *Angew. Chem.* **2009**, *121*, 4450 – 4453; *Angew. Chem. Int. Ed.* **2009**, *48*, 4386 – 4389.
[15] Y. Y. Shao, J. Liu, Y. Wang, Y. H. Lin, *J. Mater. Chem.* **2009**, *19*, 46 – 59.
[16] K. Wiesener, *Electrochim. Acta* **1986**, *31*, 1073 – 1078.
[17] K. Sawai, D. Uda, *Chem. Lett.* **2006**, *35*, 1166 – 1167.
[18] K. Sawai, D. Uda, K. Shirai, *Electrochemistry* **2007**, *75*, 163 – 165.
[19] R. Jasinski, *Nature* **1964**, *201*, 1212 – 1213.
[20] R. Bashyam, P. Zelenay, *Nature* **2006**, *443*, 63 – 66.
[21] M. Lefevre, E. Proietti, F. Jaouen, J.-P. Dodelet, *Science* **2009**, *324*, 71 – 74.
[22] M. N. Zhang, Y. M. Yan, K. P. Gong, L. Q. Mao, Z. X. Guo, Y. Chen, *Langmuir* **2004**, *20*, 8781 – 8785.
[23] I. Kruusenberg, L. Matisen, H. Jiang, M. Huuppola, K. Kontturi, K. Tammeveski, *Electrochem. Commun.* **2010**, *12*, 920 – 1923.
[24] Y. Tang, B. L. Allen, D. R. Kauffman, A. Star, *J. Am. Chem. Soc.* **2009**, *131*, 13200.
[25] R. K. Lee, U. K. Lee, J. W. Lee, B. T. Ahn, S. I. Woo, *Electrochem. Commun.* **2010**, *12*, 1052 – 1055.
[26] N. Alexeyeva, E. Shulga, V. Kisand, I. Kink, K. Tammeveski, *J. Electroanal. Chem.* **2010**, *648*, 169.
[27] P. H. Matter, L. Zhang, U. S. Ozkan, *J. Catal.* **2006**, *239*, 83.
[28] P. H. Matter, E. Wang, M. Arias, E. J. Biddinger, U. S. Ozkan, *J. Phys. Chem. B* **2006**, *110*, 18374.
[29] F. Tuinstra, J. L. Koenig, *J. Chem. Phys.* **1970**, *53*, 1126.
[30] T. Ohsaka, L. Mao, K. Arihara, T. Sotomura, *Electrochem. Commun.* **2004**, *6*, 273.
[31] V. V. Strelko, V. S. Kuts, P. A. Thrower, *Carbon* **2000**, *38*, 1499.
[32] U. A. Paulus, A. Wokaun, G. G. Scherer, T. J. Schmidt, V. Stamenkovic, V. Radmilovic, N. M. Markovic, P. N. Ross, *J. Phys. Chem. B* **2002**, *106*, 4181.
[33] Y. Y. Shao, G. P. Yin, Y. Z. Gao, *J. Power Sources* **2007**, *171*, 558.

